

Reactivity of NO₂ with Porous and Conductive Copper Azobispyridine Metallopolymers

Naomi E. Clayman,^{†,⊥} Mary Anne Manumpil,^{†,⊥} Benjamin D. Matson,^{†,§} Shengkai Wang,[‡] Adam H. Slavney,[†] Ritimuka Sarangi,^{*,§} Hemamala I. Karunadasa,^{*,†} and Robert M. Waymouth^{*,†}

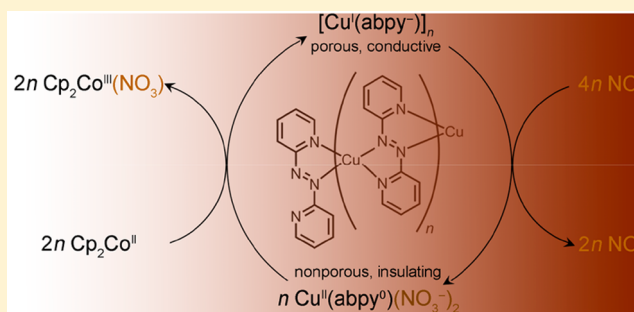
[†]Department of Chemistry, Stanford University, Stanford, California 94305, United States

[‡]Department of Mechanical Engineering, Stanford University, Stanford, California 94305, United States

[§]Stanford Synchrotron Radiation Lightsource, SLAC National Accelerator Laboratory, Menlo Park, California 94025, United States

Supporting Information

ABSTRACT: We report the reactivity of copper azobispyridine (abpy) metallopolymers with nitrogen dioxide (NO₂). The porous and conductive [Cu(abpy)]_n mixed-valence metallopolymers undergo a redox reaction with NO₂, resulting in the disproportionation of NO₂ gas. Solid- and gas-phase vibrational spectroscopy and X-ray analysis of the reaction products of the NO₂-dosed metallopolymer show evidence of nitrate ions and nitric oxide gas. Exposure to NO₂ results in complete loss of porosity and a decrease in the room-temperature conductivity of the metallopolymer by four orders of magnitude with the loss of mixed-valence character. Notably, the porous and conductive [Cu(abpy)]_n metallopolymers can be reformed by reducing the Cu-nitrate species.



INTRODUCTION

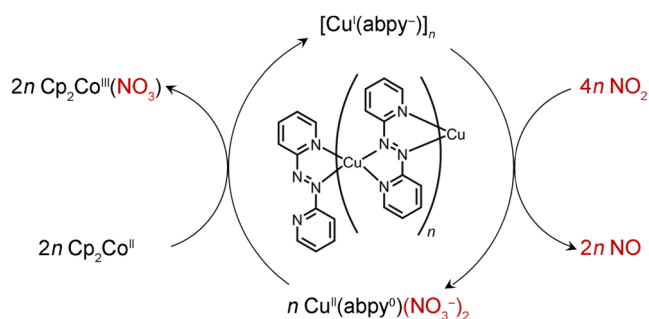
Combustion of fossil fuels that powers much of the transportation and industry in today's society results in the release of toxic gases into the atmosphere. Among these gases is NO₂, a dangerous brown gas found in smog. Continued exposure to low concentrations (~1 ppm) of NO₂ can result in chronic respiratory problems; short-term exposure to 10 ppm induces acute respiratory difficulties, and concentrations nearing 100 ppm can result in death.¹ These biological and environmental concerns have motivated studies to identify materials that can sense or react with and capture NO₂.^{1–5} Sensor technologies have been developed to detect small amounts of NO₂ gas.^{1–5} Materials that react with NO₂ without interfering reactions with more abundant gaseous species (N₂, O₂, CO₂) also have potential environmental applications for the capture and sequestration of these toxic gases.

We previously described⁶ the electrically conductive and porous copper azobispyridine (abpy) metallopolymers [Cu(abpy)]_n. These metallopolymers exhibit an unusual combination of substantial conductivity (0.18 S·cm⁻¹ at room temperature) and porosity (90 m²·g⁻¹). The conductivity of the neutral polymer, with oxidation states formally assigned as [Cu⁺(abpy^{-•})]_n, was attributed to its mixed-valence character.⁶ The [Cu(abpy)]_n metallopolymer can be reversibly oxidized at -0.8 V vs Ag/AgNO₃ to the insulating (<10⁻¹⁰ S·cm⁻¹) and nonporous cationic metallopolymer, formally assigned as [Cu⁺(abpy⁰)X]_n (X = monoanion). As a reducing, porous

material, we anticipated that the neutral metallopolymer might react with oxidizing gases such as NO₂.

Herein, we report the reaction of the porous and conductive [Cu(abpy)]_n with NO₂ gas (Scheme 1). This gas/solid redox

Scheme 1. Proposed Reaction of [Cu(abpy)]_n with NO₂ Gas



reaction results in oxidation of the metallopolymer and the reductive disproportionation of NO₂ gas into nitric oxide (NO) gas and nitrate anions (NO₃⁻). Notably, after exposure to NO₂ gas, the resulting oxidized material can be reduced to regenerate [Cu(abpy)]_n with approximately 75% recovery of the porosity and conductivity of the original metallopolymer.

Received: April 23, 2019

RESULTS AND DISCUSSION

Metallopolymer $[\text{Cu}(\text{abpy})]_n$, generated from the chemical reduction of $[\text{Cu}(\text{abpy})\text{PF}_6]_n$ with Cp_2Co ,⁶ was used for all NO_2 reactivity studies. Black powders of $[\text{Cu}(\text{abpy})]_n$ were dosed with either a mixture of NO_2 (1%) in dry air (99%) or a mixture of NO_2 (2%) in dry N_2 (98%) at room temperature for variable amounts of time. Solid $[\text{Cu}(\text{abpy})]_n$ is insoluble in water and organic solvents. After exposure to NO_2 , the resulting green powders become soluble in most polar organic solvents such as acetonitrile (CH_3CN) to afford a dark purple/black solution. Analysis of the headspace of a sample of $[\text{Cu}(\text{abpy})]_n$ after exposure to an atmosphere of 2% NO_2 in N_2 reveals the presence of NO gas (approximately 0.6 mol %; Figure 1), as determined by mid-IR tunable diode laser

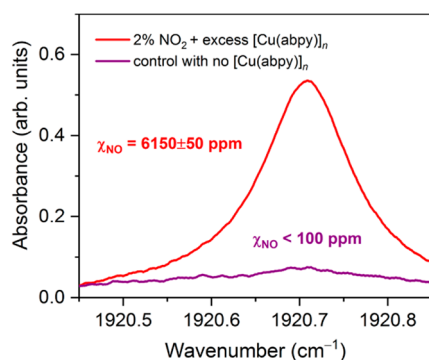
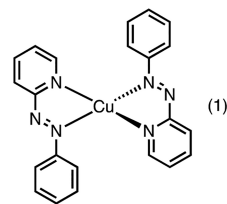


Figure 1. Mid-IR laser absorption analysis of the gas product of $[\text{Cu}(\text{abpy})]_n$ dosed with NO_2 (red). The strong characteristic absorption of NO appears near 1920.71 cm^{-1} . In this example, the final NO mole fraction in the reactor headspace was determined to be 6150 ppm. As a control, the 2% NO_2/N_2 mixture was also introduced to the reactor without $[\text{Cu}(\text{abpy})]_n$ (purple). The background NO mole fraction, determined from this control test, was less than 100 ppm.

absorption near 1920 cm^{-1} . The evolution of NO gas is very fast, occurring within the first 0.2 s of NO_2 exposure. Under the conditions used for monitoring, the NO concentration in the reaction headspace reaches about 0.2 mol % in the first 0.2 s (Figure S1).

Several experiments were carried out to identify the other nitrogen oxides generated from the reaction of the metallopolymer $[\text{Cu}(\text{abpy})]_n$ with NO_2 . The reaction products were dissolved in CH_3CN and analyzed by electrospray-ionization mass spectrometry (ESI-MS, see Supporting Information). The most intense peak in the spectrum in negative mode is an ion at 61 m/z , corresponding to NO_3^- (Figure S2). Of the ions observed in positive mode, one corresponds to $\text{Cu}(\text{abpy})_2^+$ (431 m/z , Figure S3), indicating fragmentation of the polymer chain upon exposure to NO_2 . We also observe adducts of copper, azobispyridine ligand, and NO_3^- . The ESI-MS indicates that $[\text{Cu}(\text{abpy})]_n$ is oxidized by NO_2 , and the copper speciates as a NO_3^- adduct. No nitrate is observed in the ESI-MS of acetonitrile saturated with 2% NO_2 in N_2 .

To better understand the metallopolymer's reactivity with NO_2 , we carried out similar studies with $(\text{Cu}(\text{azpy})_2)$ (1) (azpy = phenylazo-2-pyridine), a molecular analogue of $[\text{Cu}(\text{abpy})]_n$ where one pyridyl ring per Cu center is replaced by a phenyl ring to prevent bridging to another Cu center. Here, the ligand-based mixed valence is formally designated as $\text{Cu}^+(\text{azpy}^{0.5-})_2$.⁶ Before exposure of $\text{Cu}(\text{azpy})_2$ to NO_2 , the



major ion observed in positive mode exhibited an m/z value of 429, corresponding to $\text{Cu}(\text{azpy})_2^+$ (Figure S4). After exposure of powders of $\text{Cu}(\text{azpy})_2$ to NO_2 gas, the ESI-MS spectrum of $\text{Cu}(\text{azpy})_2$ changes. A new ion with a m/z of 491, corresponding to $[\text{Cu}(\text{azpy})_2\text{NO}_3]^+$, emerges (Figure S5), in addition to an ion at 308 m/z , corresponding to the formation of $[\text{Cu}(\text{azpy})\text{NO}_3]^+$ (Figure S6). Fragmentative collision-induced dissociation (CID) performed on the ion at 491 m/z resulted in the loss of one of the azpy ligands, and the complex fragmented into $[\text{Cu}^{2+}(\text{azpy}^0)\text{NO}_3]^+$. This observation implies that the nitrate anion is coordinated to the Cu^{II} center and is more strongly bound to the metal center than one of the azpy ligands. This strong coordination of nitrate could facilitate the fragmentation of the polymer chain upon NO_2 exposure.

Reduction of the powder obtained through exposure of $[\text{Cu}(\text{abpy})]_n$ to NO_2 gas with cobaltocene (Cp_2Co) results in the precipitation of a black solid and yellow supernatant. Slow vapor diffusion of pentane into the dichloromethane/ CH_3CN supernatant held at $-20\text{ }^\circ\text{C}$ afforded yellow needles of cobaltocenium nitrate ($\text{Co}^{\text{III}}\text{Cp}_2\text{NO}_3$; $\text{Cp} = \text{C}_5\text{H}_5^-$) as confirmed by single-crystal X-ray diffraction (Figure S8). The isolation of a nitrate salt further verifies the oxidation of NO_2 to NO_3^- by the metallopolymer. We obtained crystals of $\text{Co}^{\text{III}}\text{Cp}_2\text{NO}_3$ regardless of whether the reaction with NO_2 was performed in dry air or dry N_2 . The crystallization of Cp_2CoNO_3 under O_2 -free conditions indicates that all three oxygen atoms in NO_3^- originate from the NO_2 and not from O_2 . Confirmation of the origin of the oxygen atoms in NO_3^- was obtained by IR spectroscopy analysis of three samples of $[\text{Cu}(\text{abpy})]_n$ dosed with different gas mixtures: one was dosed with only 2% NO_2 in N_2 , one with 2% NO_2 in N_2 and codosed with $^{16}\text{O}_2$, and one codosed with $^{18}\text{O}_2$. The IR spectra of all three samples (Figure S9) are identical: no differences could be observed for samples with and without oxygen exposure, and no isotopic shifts were observed in any peaks when $^{18}\text{O}_2$ was introduced into the system, confirming that the oxygens in NO_3^- are derived from NO_2 .

We probed the solid-phase–gas-phase reaction between $[\text{Cu}(\text{abpy})]_n$ and NO_2 by a variety of spectroscopic techniques. Powders of $[\text{Cu}(\text{abpy})]_n$ display a broad absorbance around $\sim 2500\text{ cm}^{-1}$ in the mid-infrared region (Figure S10).⁶ This absorbance is the low-energy tail of the band we assign as a predominantly ligand-based intervalence charge transfer (IVCT)⁷ band. This IVCT band is absent in the IR spectrum of $[\text{Cu}(\text{abpy})]_n$ after NO_2 dosing (Figure S10), suggesting that the product no longer possesses radical abpy ligands. Upon NO_2 dosing, we also observe the emergence of a new peak at 1273 cm^{-1} (Figure S10), which has been previously attributed to coordinated nitrate (NO_3^-) in anhydrous cupric nitrate.⁸

Changes in electronic structure after NO_2 exposure were observed by electron paramagnetic resonance (EPR) spectroscopy. The EPR spectrum of $[\text{Cu}(\text{abpy})]_n$ features a broad peak with a g value of 2.08, corresponding to radical abpy ligands with possible contribution from the copper centers due to electronic delocalization.⁶ The solid-state EPR spectrum of

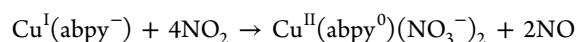
$[\text{Cu}(\text{abpy})]_n$ after 16 h of NO_2 (2%) exposure reveals that this broad, symmetrical signal in $[\text{Cu}(\text{abpy})]_n$ diminishes upon exposure to NO_2 . We also observe the emergence of a new signal with characteristic rhombic Cu^{II} spectral shape (Figure S12A).⁹ There is literature precedent for disproportionation of NO_2 on electron-rich surfaces, and in fact, Addison et al.¹⁰ report the isolation of $\text{Cu}^{\text{II}}(\text{NO}_3)_2$ and NO gas when copper metal is treated with NO_2 in the form of liquid N_2O_4 .

Cu K-edge X-ray absorption spectroscopy (XAS) was used to further evaluate the oxidation state of Cu in samples of $[\text{Cu}(\text{abpy})]_n$ before and after NO_2 dosing, as well as in $[\text{Cu}(\text{abpy})\text{PF}_6]_n$. The Cu K rising edge region is dominated by Cu $1s \rightarrow 4p+$ continuum transitions (~ 8979 eV) and is therefore strongly modulated by the effective nuclear charge (Z_{eff}) on Cu.^{11–14} The rising edge of $[\text{Cu}(\text{abpy})\text{PF}_6]_n$, measured as the maximum of the first derivative, occurs at an energy of 8982.6 eV and is very similar in energy and shape to that of the molecular model compound $[\text{Cu}(\text{azpy})_2][\text{PF}_6]_n$,¹⁵ which has a slightly higher rising edge energy of 8983.4 eV.

The rising edge of both $[\text{Cu}(\text{abpy})\text{PF}_6]_n$ and $[\text{Cu}(\text{azpy})_2][\text{PF}_6]_n$ occur at an energy higher than that of $[\text{Cu}(\text{bpy})_2][\text{PF}_6]$ (bpy = 2,2'-bipyridine), indicating an increase in Z_{eff} on Cu as the bipyridine ligand is replaced with more redox-active azpy or abpy ligands, indicating that $[\text{Cu}(\text{abpy})\text{PF}_6]_n$ is better represented as $[\text{Cu}^{1+\delta}(\text{abpy}^{-\delta})\text{PF}_6]_n$. The rising edge of the reduced species $[\text{Cu}(\text{abpy})]_n$ shows a distinct change in shape with a slight increase in rising edge energy (8982.9 eV, Figure 2A). Remarkably, this shift in rising edge energy is indicative of an increase in the Z_{eff} on Cu upon reduction of $[\text{Cu}(\text{abpy})-$

$\text{PF}_6]_n$; the Cu metal centers appear to be more oxidized after a bulk reduction of the material, resulting in $[\text{Cu}^{1+\Delta}(\text{abpy}^{-(1+\Delta)})]_n$, where $\Delta > \delta$. Although rare, a similar phenomenon has been observed in molybdenum and tungsten compounds with sulfur-based redox noninnocent ligands, wherein a net oxidation of the compound resulted in a reduction of the metal center.^{16–19} Dosing $[\text{Cu}(\text{abpy})]_n$ with NO_2 results in a dramatic blue-shifting of the rising edge energy to 8986.2 eV. Thus, the reaction of $[\text{Cu}(\text{abpy})]_n$ with NO_2 yields copper species with rising edge energies similar to that of the $\text{Cu}^{\text{II}}(\text{bpy})_2(\text{BF}_4)_2$ (8986.3 eV, Figure 2B), indicating that the oxidation states of the products of NO_2 exposure are most reasonably formulated as Cu^{II} species.

Combining evidence from IR spectroscopy, EPR, and XAS, we propose that $[\text{Cu}(\text{abpy})]_n$ reacts with four equivalents of NO_2 gas per copper center, where NO_2 oxidizes both the Cu and the abpy ligand and disproportionates to form NO_3^- and NO . Although approximate oxidation state assignments are given below, we note that there is considerable electronic delocalization between Cu and the abpy ligand, as discussed above:



Solid $[\text{Cu}(\text{abpy})]_n$ has a room-temperature conductivity of $0.18 \text{ S}\cdot\text{cm}^{-1}$, which increases up to $0.46 \text{ S}\cdot\text{cm}^{-1}$ upon heating to 125°C , and an activation energy for conduction of 98 meV.^{6,20} Upon exposing powders of $[\text{Cu}(\text{abpy})]_n$ to NO_2 (2%) for 1 h, the room-temperature conductivity of the material drops to $8.5 \times 10^{-2} \text{ S}\cdot\text{cm}^{-1}$. After 16 h of exposure, the room-temperature conductivity value decreases to $6.4 \times 10^{-5} \text{ S}\cdot\text{cm}^{-1}$. Likewise, the activation energy increases up to 290 meV upon NO_2 dosing. Electrical conductivity in $[\text{Cu}(\text{abpy})]_n$ is thought to arise from electron hopping between radical mixed-valence abpy ligands.⁶ From the EPR and IR spectra, we infer that the redox reaction between NO_2 and $[\text{Cu}(\text{abpy})]_n$ results in a loss of mixed valency. A decrease in conductivity upon NO_2 exposure is consistent with this interpretation and confirms the loss of electronic communication across the material.

We also observe changes in the surface area of $[\text{Cu}(\text{abpy})]_n$ upon NO_2 exposure. Fine powders of $[\text{Cu}(\text{abpy})]_n$ have a Brunauer–Emmett–Teller (BET) surface area of $90 \text{ m}^2\cdot\text{g}^{-1}$.⁶ Concomitant with loss of conductivity, we also observe a complete loss of porosity after NO_2 dosing for 16 h (Figure 3). The observed lack of porosity in NO_2 -dosed $[\text{Cu}(\text{abpy})]_n$ is

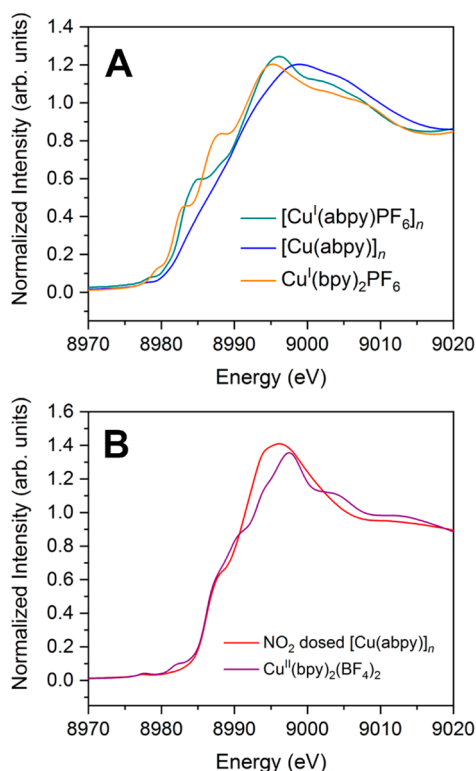


Figure 2. Normalized Cu–K edge XAS spectra of (A) $[\text{Cu}^{\text{I}}(\text{abpy})\text{PF}_6]_n$ (teal), $[\text{Cu}(\text{abpy})]_n$ (blue), and $\text{Cu}^{\text{I}}(\text{bpy})_2\text{PF}_6$ (bpy = 2,2'-bipyridine; orange), a Cu^{I} standard, and (B) $\text{Cu}^{\text{II}}(\text{bpy})_2(\text{BF}_4)_2$ (purple), a Cu^{II} standard, and $[\text{Cu}(\text{abpy})]_n$ after exposure to NO_2 gas for 24 h (red).

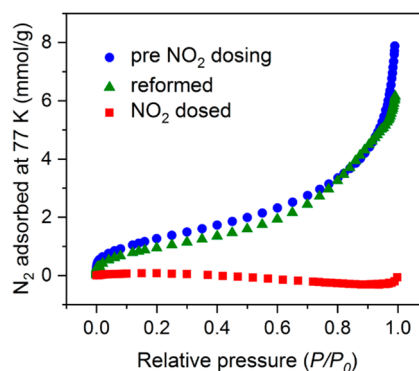


Figure 3. Nitrogen isotherms measured at 77 K of $[\text{Cu}(\text{abpy})]_n$ before exposure to NO_2 gas (blue), after NO_2 exposure (red), and after regeneration of the material by Cp_2Co reduction (green). Surface areas are $90 \text{ m}^2/\text{g}$, $\sim 0 \text{ m}^2/\text{g}$, and $70 \text{ m}^2/\text{g}$, respectively.

consistent with the oxidation of the material to a cationic species associated with NO_3^- anions and likely also to the fragmentation of the polymer chains upon gas exposure.

As the reaction between $[\text{Cu}(\text{abpy})]_n$ and NO_2 is a redox reaction, we sought to regenerate $[\text{Cu}(\text{abpy})]_n$ from the oxidized product using a chemical reductant. The addition of a solution of Cp_2Co to a solution of the polymer after exposure to NO_2 results in the isolation of black powders with properties reminiscent of $[\text{Cu}(\text{abpy})]_n$. Inductively coupled plasma atomic emission spectroscopy (ICP-AES) and combustion analysis reveal that the approximate formula of the black powders is $[\text{Cu}(\text{abpy})]_n$ (see Supporting Information). The solid-state EPR spectrum of the reformed polymer shows a broad peak with a g value of 2.08, similar to that of $[\text{Cu}(\text{abpy})]_n$ (Figure S13).

To confirm that we successfully regenerated the $[\text{Cu}(\text{abpy})]_n$ polymer's properties upon chemical reduction after exposure to NO_2 , we measured the optical, electronic, and gas sorption properties of the reformed material. The fingerprint region of the IR spectrum of the reformed material matches that of the original polymer (Figure S14). Significantly, we observe the return of the low-energy tail of the IVCT band in the IR spectrum that disappeared upon NO_2 exposure. The re-emergence of the IVCT indicates the reformation of radical abpy ligands upon reduction.

The regenerated material has a room-temperature conductivity ($7.8 \times 10^{-2} \text{ S}\cdot\text{cm}^{-1}$) and an activation energy for conductivity (160 meV) similar to that of $[\text{Cu}(\text{abpy})]_n$ generated from $[\text{Cu}(\text{abpy})\text{PF}_6]_n$ ($0.18 \text{ S}\cdot\text{cm}^{-1}$ and 98 meV, respectively). Furthermore, we find that the regenerated material regains a significant fraction of the porosity with a BET surface area of $70 \text{ m}^2\cdot\text{g}^{-1}$ (vs $90 \text{ m}^2\cdot\text{g}^{-1}$ for $[\text{Cu}(\text{abpy})]_n$). We have shown that the porosity of $[\text{Cu}(\text{abpy})]_n$ arises from expulsion of charge-balancing anions upon reduction of the $[\text{Cu}(\text{abpy})\text{X}]_n$ ($\text{X} = \text{Br}^-, \text{PF}_6^-, \text{BAR}_4^{\text{F}-}$) from which it is generated.⁶ The slightly lower conductivities and surface areas of the regenerated materials may be due to the templating effect mediated by the extrusion of different anions (NO_3^- vs PF_6^-) upon reduction. To test this hypothesis, we prepared a sample of $[\text{Cu}(\text{abpy})]_n$ from $[\text{Cu}(\text{abpy})\text{NO}_3]_n$ to see if the porosity of the reformed material can be attributed to the anion templating effect. Reduction of $[\text{Cu}(\text{abpy})\text{NO}_3]_n$ yields $[\text{Cu}(\text{abpy})]_n$ with a BET surface area of $60 \text{ m}^2\cdot\text{g}^{-1}$ (Figure S15).

The lower porosity of the $[\text{Cu}(\text{abpy})]_n$ generated from $[\text{Cu}(\text{abpy})\text{NO}_3]_n$ compared to that generated from $[\text{Cu}(\text{abpy})\text{PF}_6]_n$ is consistent with the previously observed templating effect because PF_6^- is larger than NO_3^- .⁶ Because we expect the polymer to fragment upon NO_3^- coordination to the Cu centers, this templating effect may not be as strong when reforming $[\text{Cu}(\text{abpy})]_n$ from the NO_2 reaction product mixture. The $10 \text{ m}^2\cdot\text{g}^{-1}$ difference in surface area between the $[\text{Cu}(\text{abpy})]_n$ polymer generated from $[\text{Cu}(\text{abpy})\text{NO}_3]_n$ and the $[\text{Cu}(\text{abpy})]_n$ polymer reformed from the NO_2 reaction may also be within experimental error as the surface area of these soft materials is very sensitive to handling conditions.⁶

CONCLUSIONS

In conclusion, we report the reactivity of the porous and electrically conductive copper azobispyridine metallopolymer, $[\text{Cu}(\text{abpy})]_n$, with NO_2 . Intriguingly, XAS analysis indicates that the oxidation state of the copper ions *increases* upon reduction of $[\text{Cu}(\text{abpy})\text{PF}_6]_n$ to generate $[\text{Cu}(\text{abpy})]_n$,

indicating that the abpy ligands are actively engaged in the redox reactions of these materials. The redox reaction between NO_2 and $[\text{Cu}(\text{abpy})]_n$ results in the disproportionation of NO_2 into nitrate and NO gas, as evidenced by vibrational spectroscopy and single-crystal X-ray diffraction. EPR and XAS provide evidence for the oxidation of both the ligand and the copper center upon reaction of $[\text{Cu}(\text{abpy})]_n$ with NO_2 . Upon exposure to NO_2 , the metallopolymer's room-temperature conductivity value drops by four orders of magnitude as it loses its mixed-valence character. Additionally, NO_2 dosing causes the metallopolymers to completely lose porosity. Lastly, $[\text{Cu}(\text{abpy})]_n$ metallopolymers can be regenerated after oxidation by NO_2 by chemical reduction, recovering much of the electrical conductivity, porosity, and optical properties of the parent polymer. These promising findings make $[\text{Cu}(\text{abpy})]_n$ a good platform for developing materials for NO_2 sensing and sequestration.

ASSOCIATED CONTENT

Supporting Information

The Supporting Information is available free of charge on the ACS Publications website at DOI: 10.1021/acs.inorgchem.9b01190.

Experimental descriptions, synthetic procedures, and material characterization (PDF)

AUTHOR INFORMATION

Corresponding Authors

*E-mail: waymouth@stanford.edu.

*E-mail: hemamala@stanford.edu.

*E-mail: ritis@slac.stanford.edu.

ORCID

Naomi E. Clayman: 0000-0002-4894-2174

Benjamin D. Matson: 0000-0001-5733-0893

Shengkai Wang: 0000-0003-0947-4643

Ritimuka Sarangi: 0000-0002-2764-2279

Hemamala I. Karunadasa: 0000-0003-4949-8068

Robert M. Waymouth: 0000-0001-9862-9509

Author Contributions

¹N.E.C and M.A.M. contributed equally.

Notes

The authors declare no competing financial interest.

ACKNOWLEDGMENTS

N.E.C. and R.M.W. thank the Office of Naval Research (ONR N000141410551) and the Center for Molecular Analysis and Design (CMAD) for a graduate fellowship. Work by M.A.M., A.H.S, and H.I.K. was funded by an NSF CAREER award (DMR-1351538). M.A.M. thanks CMAD, the National Science Foundation (NSF; award DGE-114747), and Stanford's Diversifying Academia, Recruiting Excellence Program for fellowships. B.D.M. was supported by the Precourt Institute for Energy (2017-4-Waymouth). Use of the Stanford Synchrotron Radiation Lightsource, SLAC National Accelerator Laboratory, is supported by the U.S. Department of Energy, Office of Science, Office of Basic Energy Sciences under Contract DE-AC02-76F00515. Single crystal X-ray diffraction was performed on Beamline 11.3.1 at the Advanced Light Source, which is a DOE Office of Science User Facility under Contract DE-AC02-05CH11231. We thank Prof. Matteo Cargnello and Dr. Michael Aubrey for

helpful discussions. We thank Dr. Abraham Saldivar Valdes, Dr. Michael Aubrey, Dr. Matthew D. Smith, Kurt Lindquist, and Katherine Walker for experimental assistance. We thank Prof. Edward I. Solomon and Prof. Ronald K. Hanson for access to equipment. XAS measurements were performed at beamline 7-3 at the Stanford Synchrotron Radiation Light-source (SSRL).

REFERENCES

- (1) Huang, W.; Zhuang, X.; Melkonyan, F. S.; Wang, B.; Zeng, L.; Wang, G.; Han, S.; Bedzyk, M. J.; Yu, J.; Marks, T. J.; Facchetti, A. UV–Ozone Interfacial Modification in Organic Transistors for High-Sensitivity NO₂ Detection. *Adv. Mater.* **2017**, *29*, 1701706.
- (2) Pearce, R.; Iakimov, T.; Andersson, M.; Hultman, L.; Spetz, A. L.; Yakimova, R. Epitaxially grown graphene based gas sensors for ultra sensitive NO₂ detection. *Sens. Actuators, B* **2011**, *155*, 451–455.
- (3) Ferroni, M.; Guidi, V.; Martinelli, G.; Sacerdoti, M.; Nelli, P.; Sberveglieri, G. MoO₃-based sputtered thin films for fast NO₂ detection. *Sens. Actuators, B* **1998**, *48*, 285–288.
- (4) Xia, H.; Wang, Y.; Kong, F.; Wang, S.; Zhu, B.; Guo, X.; Zhang, J.; Wang, Y.; Wu, S. Au-doped WO₃-based sensor for NO₂ detection at low operating temperature. *Sens. Actuators, B* **2008**, *134*, 133–139.
- (5) Andringa, A.-M.; Piliago, C.; Katsouras, I.; Blom, P. W. M.; de Leeuw, D. M. NO₂ Detection and Real-Time Sensing with Field-Effect Transistors. *Chem. Mater.* **2014**, *26*, 773–785.
- (6) Clayman, N. E.; Manumpil, M. A.; Umeyama, D.; Rudenko, A. E.; Karunadasa, H. I.; Waymouth, R. M. Carving Out Pores in Redox-Active One-Dimensional Coordination Polymers. *Angew. Chem., Int. Ed.* **2018**, *57*, 14585–14588.
- (7) D'Alessandro, D. M.; Keene, F. R. Current trends and future challenges in the experimental, theoretical and computational analysis of intervalence charge transfer (IVCT) transitions. *Chem. Soc. Rev.* **2006**, *35*, 424–440.
- (8) Addison, C. C.; Gatehouse, B. M. The Infrared Spectra of Anhydrous Transition-metal Nitrates. *J. Chem. Soc.* **1960**, 613–616.
- (9) Garribba, E.; Micera, G. The Determination of the Geometry of Cu(II) Complexes: An EPR Spectroscopy Experiment. *J. Chem. Educ.* **2006**, *83*, 1229–1232.
- (10) Addison, C. C. Dinitrogen Tetroxide, Nitric Acid, and Their Mixtures as Media for Inorganic Reactions. *Chem. Rev.* **1980**, *80*, 21–39.
- (11) Cho, J.; Sarangi, R.; Kang, H. Y.; Lee, J. Y.; Kubo, M.; Ogura, T.; Solomon, E. I.; Nam, W. Synthesis, Structural, and Spectroscopic Characterization and Reactivities of Mononuclear Cobalt(III)–Peroxo Complexes. *J. Am. Chem. Soc.* **2010**, *132*, 16977–16986.
- (12) Sarangi, R. X-ray absorption near-edge spectroscopy in bioinorganic chemistry: Application to M–O₂ systems. *Coord. Chem. Rev.* **2013**, *257*, 459–472.
- (13) Sarangi, R.; Cho, J.; Nam, W.; Solomon, E. I. XAS and DFT Investigation of Mononuclear Cobalt(III) Peroxo Complexes: Electronic Control of the Geometric Structure in CoO₂ versus NiO₂ Systems. *Inorg. Chem.* **2011**, *50*, 614–620.
- (14) DuBois, J. L.; Mukherjee, P.; Stack, T. D. P.; Hedman, B.; Solomon, E. I.; Hodgson, K. O. A Systematic K-edge X-ray Absorption Spectroscopic Study of Cu(III) Sites. *J. Am. Chem. Soc.* **2000**, *122*, 5775–5787.
- (15) Datta, D.; Chakravorty, A. Bis(2-(phenylazo)pyridine)copper(I) and -copper(II): Ligand π Acidity and High Formal Potential of the Copper(II)-Copper(I) Couple. *Inorg. Chem.* **1983**, *22*, 1085–1090.
- (16) Stiefel, E. I.; Halbert, T. R.; Coyle, C. L.; Wei, L.; Pan, W.-H.; Ho, T. C.; Chianelli, R. R.; Daage, M. Molecules, clusters, solids and catalysts in early transition metal sulphide systems. *Polyhedron* **1989**, *8*, 1625–1629.
- (17) Yang, X.; Freeman, G. K. W.; Rauchfuss, T. B.; Wilson, S. R. Dithiocarbonate route to 1,2-dithiolene complexes of molybdenum and tungsten. *Inorg. Chem.* **1991**, *30*, 3034–3038.
- (18) Coyle, C. L.; Harmer, M. A.; George, G. N.; Daage, M.; Stiefel, E. I. Conversion of [MoS₄]²⁻ to [Mo₂S₂(μ -S)₂(S₂)₂]²⁻ by Organic Disulfides: The Mechanism of an Induced Redox Reaction. *Inorg. Chem.* **1990**, *29*, 14–19.
- (19) Sarkar, S.; Ansari, M. A. Conversion of WOS₃²⁻ into [W₂O₂(μ -S)₂(S₂)₂]²⁻ and *vice-versa* by internal redox processes induced by I₂ and S_x²⁻. *J. Chem. Soc., Chem. Commun.* **1986**, 324–325.
- (20) Shao, Q.; Jiang, S. Effect of Carbon Spacer Length on Zwitterionic Carboxybetaines. *J. Phys. Chem. B* **2013**, *117*, 1357–1366.